Ab initio calculation of phonon dispersions in size-mismatched disordered alloys

Biswanath Dutta,* Konark Bisht,† and Subhradip Ghosh‡
Department of Physics, Indian Institute of Technology Guwahati, Guwahati, Assam 781039, India
(Received 12 June 2010; revised manuscript received 4 August 2010; published 13 October 2010)

Size mismatch and the resulting local lattice relaxations play a very crucial role in determining the lattice-dynamical properties of substitutionally disordered alloys. In this paper we focus on the influence of size mismatch between the components of a disordered alloy on the phonon dispersions, by considering the illustrative examples of $Cu_{0.715}Pd_{0.285}$ and $Cu_{0.75}Au_{0.25}$ systems. A combination of *ab initio* electronic-structure method and the transferable force-constant model has been used as a first-principles tool to compute the interatomic force constants between various pairs of chemical specie in a disordered alloy. The Green's-function based itinerant coherent-potential approximation is then used to compute the phonon-dispersion relations by performing the configuration averaging over the fluctuations in the mass and the force constants due to the size mismatch. A systematic investigation on the influence of the size mismatch of end-point components of an alloy on the phonon spectra is carried out in detail. We show that the consideration of the local lattice relaxation as a manifestation of size mismatch is important in addressing the correct behavior of the phonon dispersions in these alloys. Our results are in good agreement with the experimental results in case of $Cu_{0.715}Pd_{0.285}$. In case of $Cu_{0.75}Au_{0.25}$, our results predict a resonance behavior which is not observed experimentally. Based upon an analysis of the interatomic force constants between various pairs of chemical specie, we explain the reason of this discrepancy.

DOI: 10.1103/PhysRevB.82.134207 PACS number(s): 63.20.dk, 63.50.Gh

I. INTRODUCTION

Study of phonon excitations in solids offer interesting perspectives regarding materials properties and behavior.[1] Useful insight about the ordering behavior, phase stability and elastic properties, to name a few, can be obtained from the phonon-dispersion relations of solids. The microscopic understanding of the material properties and the distinct phenomena in materials from their lattice dynamics require robust and accurate theoretical tools. For perfect crystals and ordered alloys, the theory of lattice vibrations has been setup on a rigorous basis. However, the same is not true for substitutionally disordered alloys. The presence of disorder results in scattering that not only depends on the impurity concentration but also crucially on both the relative mass and size differences between the constituent atoms.[2–4] Novel features in the phonon spectra can be expected if the mass and the interatomic force constants of the impurities differ substantially from those of the host material. Prototype examples of such systems are Ni-Pt, Cu-Pd, and Cu-Au (Refs. 5–9) alloys where a significant mass as well as size ratio exists among the constituent elements. It is well known that on introduction of defects into a perfect crystal, the volume of the sample changes even in the low concentration limit of the impurity. This phenomenon of lattice relaxation is more pronounced in case of size-mismatched alloys. When atoms of different sizes are constrained to coexist on a lattice, an atom of larger (smaller) size can experience compressive (tensile) stress that results in locally stiffer (softer) regions if it is surrounded with atoms of smaller (larger) sizes. These local relaxations produce dispersions in the bond lengths associated with different pairs of chemical specie in the alloy. Correspondingly, it is expected that the stiffness of a given bond would also fluctuate depending upon the environment surrounding it. Thus, for size-mismatched alloys, three different types of disorder: the mass disorder, the force-constant disorder, and the environmental disorder; should affect the phonon-dispersion relations. A significant insight into the lattice dynamics and related properties in this class of alloys can only be gained if a microscopic picture on the role of each of the factors affecting the phonon spectra is achieved.

A substantial amount of experimental investigations have been carried out over the past few decades to understand the nature of phonon excitations in this class of alloys. Phonons are not only conceptually the simplest type of elementary excitation but are also the most readily accessible to detailed experiment. The neutron-scattering technique has yielded extremely valuable information about lattice vibrations in random alloys. However, a microscopic interpretation of these experimental observations have been rather limited due to the lack of a suitable theoretical framework which is capable of addressing all three kinds of disorders, mentioned earlier, in a *first-principles* way. Recently, a breakthrough has been possible with the advent of the Green's-function based self-consistent itinerant coherent-potential approximation (ICPA) (Ref. 10) which addresses all three kind of disorders by a suitable cluster generalization of the mean-field single-site CPA.[11] Although the ICPA was able to illustrate the importance of the force-constant disorder with regard to the phonon spectra in disordered alloys,[12,13] the interatomic force constants used were semiempirical at the best. Very recently, the ICPA has been combined with the state-of-the-art first-principles density-functional theory[14,15] based density-functional perturbation theory (DFPT),[16] and the transferable force-constant (TFC) model[4,17–20] to construct a first-principles based computational tool to calculate the phonon dispersions in disordered alloys with arbitrary compositions. This new tool has been used to compute the phonon spectra and related properties in Fe-Pd alloys.[21] In our pursuit for a first-principles based description of lattice dynamics in disordered alloys, we were reasonably successful as our ap-

TABLE I. Properties of Cu, Pd, and Au.

	Cu	Pd	Au
Atomic number	29	46	79
Atomic mass (amu)	63.55	106.4	196.9
Atomic radius (pm)	128	137	144
Nearest neighbor force Constants (dyn/cm)			
1XX	13160[a]	19337[a]	16610[b]
1XY	14880[a]	22423[a]	19930[b]
1ZZ	−1489[a]	−2832[a]	−6650[b]

[a]Reference 22.
[b]Reference 23.

proach produced results which were in close agreement with the experimental findings. The novel features of this approach are that the interatomic force constants for a given specie pair can be calculated with modest computational cost and at any arbitrary composition. This is made possible by the basic premise of the TFC model which suggests that the "force constant versus bond length" relationship is transferable across different compositions for a given alloy.

In this paper, we employ the first-principles based TFC-ICPA method to investigate the effects of strong mass disorder, strong force-constant disorder, and local lattice relaxations, driven by the size mismatch among the constituents of a disordered alloy, on the phonon spectra. We have chosen Cu-Pd and Cu-Au alloys which satisfy the above criteria and are well suited for our investigation. A brief summary of their elementary properties which are relevant to our investigations are presented in Table I. The mass ratio of Pd to Cu is, $M_{Pd}/M_{Cu}=1.674$, whereas, that of Au to Cu is, $M_{Au}/M_{Cu}=3.098$. On the other hand, force constants of Pd are, on an average, 50% larger than those of Cu, while, the Au force constants are about 30% larger than those of Cu. These large mass and force-constant ratios between the various constituent elements make the above alloys potential examples of strong mass and force-constant disorder. Neutron-scattering experimental results on the phonon-dispersion relations are available for $Cu_{0.715}Pd_{0.285}$ (Refs. 6 and 7) and $Cu_{0.75}Au_{0.25}$ (Refs. 8 and 9) systems and thus we have chosen alloys with these compositions for the present study. Our motivation is to understand the features in the phonon-dispersion results based upon analysis of the role of the mass fluctuations and the fluctuations in the interatomic force constants; the later is an estimation of the stiffness of a bond connecting a pair of atoms. This in turn would validate our computational technique for addressing alloys with higher degree of all possible disorders due to chemical substitution. In the analysis of neutron-scattering experimental results on phonon dispersions, the experimentally obtained normal-mode frequencies are routinely fitted to a Born-von Karman model and the interatomic force constants are thus extracted. However, this approach never provides a correct picture of the complex interplay of interatomic forces in a disordered alloy because the model assumes an average lattice and thus neglects any fluctuations due to the presence of specie with different chemical properties. In this work, we systematically

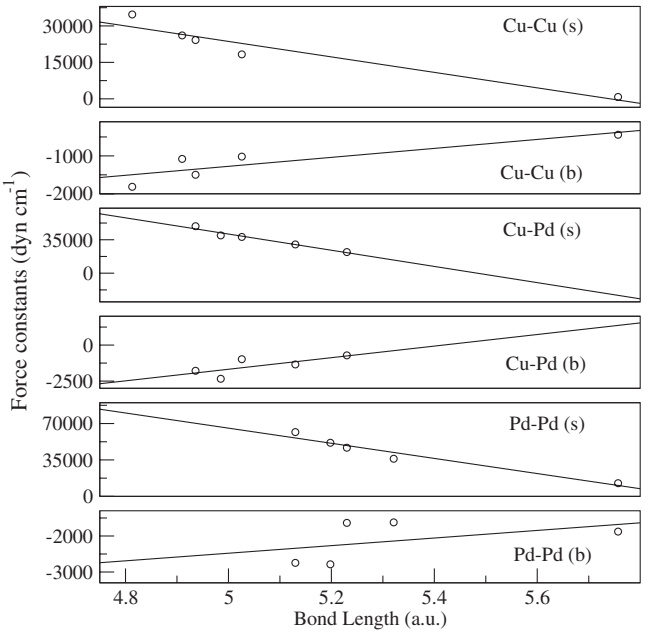

FIG. 1. Nearest-neighbor *s* and *b* force constants for Cu_xPd_{1-x} as a function of bond length. The solid lines are the fitted functions whereas the circles correspond to data obtained from *ab initio* calculations on one of a set of structures ($L1_2$ at four different volumes, $L1_0$ at two different volumes, fcc Cu and fcc Pd at two different volumes.)

show that the phonon spectra need be understood in the light of these fluctuations. Our results also show that the consideration of the local lattice relaxations is necessary in these systems. Although we get excellent agreement with the experiments for $Cu_{0.715}Pd_{0.285}$, our results significantly differ with the experiments in case of $Cu_{0.75}Au_{0.25}$. We explain the reasons behind the discrepancy in the light of the interatomic force constants and thus provide a physically reasonable picture of the microscopic situation in this system.

We organize the paper as follows. Calculation details are presented briefly in Sec. II. We skip the details of the ICPA, the TFC, and the DFPT which are discussed earlier in the literature. The subsequent section contains results and thorough discussions. Concluding remarks and future directions are presented in Sec. IV.

II. COMPUTATIONAL DETAILS

First-principles QUANTUM-ESPRESSO code,[24] based upon a plane-wave pseudopotential implementation of the DFPT,[16] has been used to compute the force constants at different bond lengths with different ordered structures. In this work, we have computed the force constants of CuPd and CuAu in different structures and at different volumes, the details of which are described in Figs. 1 and 5. Ultrasoft pseudopotentials[25] with nonlinear core corrections[26] were used. Perdew-Burke-Ernzerhof (PBE-96) generalized gradient approximation[27] functional was used for the exchange-correlation part of the potential. Plane waves with energies up to 55 Ry are used in order to describe electron wave functions and Fourier components of the augmented charge

density with cut-off energy up to 650 Ry are taken into account. The Brillouin-zone integrations are carried out with Methfessel-Paxton smearing[28] using a $14\times14\times14$ **k**-point mesh. The value of the smearing parameter is 0.02 Ry. These parameters are found to yield phonon frequencies converged to within 5%.

After achieving the desired level of convergence for the electronic structure, the force constants are conveniently computed in reciprocal space on a $4\times4\times4$ **q**-point grid and Fourier transformation is employed to obtain the real-space force constants. The resulting force constants versus bond distances data for each chemical bond is then fitted using a linear relationship according to the TFC model,

$$s(l) = s_0 + s_1(l - l_0), \tag{1}$$

$$b(l) = b_0 + b_1(l - l_0). \tag{2}$$

$s(l)$, $b(l)$ are the stretching and bending components of the force-constant tensor, respectively,[20] l_0 is the equilibrium length of a particular bond, and s_0, b_0 are the stretching and the bending components of the stiffness (force constant) of the bond at the equilibrium length, respectively. Once the transferability relation is obtained from s_1 and b_1, the interatomic force constants for a pair of atoms at any arbitrary bond length is computed.

The all-important configuration averaging is then performed by employing the ICPA method. The disorder in the force constants were considered for nearest-neighboring shell only and the calculations were done on 400 energy points. A small imaginary frequency part of −0.05 was used in the Green's function. The Brillouin-zone integration was done over 356 **q** points in the irreducible Brillouin zone. The simplest linear-mixing scheme was used to accelerate the convergence. The number of iterations ranged from 5 to 15 for all the calculations. The phonon frequencies are obtained from the peaks of the coherent scattering structure factor defined as

$$\langle\langle S_\lambda(\vec{q},w)\rangle\rangle_{coh} = \sum_{ss'} d_s d_{s'} \frac{1}{\pi} \mathrm{Im}\langle\langle G_\lambda^{ss'}(\vec{q},w^2)\rangle\rangle, \tag{3}$$

where λ is the normal-mode branch index, d_s is the coherent scattering length for the species s, and $\langle\langle G_\lambda^{ss'}(\vec{q},w^2)\rangle\rangle$ is the configuration-averaged spectral function associated with the species pair s, s'.

III. RESULTS

We discuss our results on $Cu_{0.715}Pd_{0.285}$ and $Cu_{0.75}Au_{0.25}$ in two different sections. Our calculations of the phonon-dispersion relations are compared with the available experimental results. The interpretation of our results and the agreement (discrepancy) with experimental results are done with the help of the coherent scattering structure factors.

A. $Cu_{0.715}Pd_{0.285}$

In Fig. 1, we present the stretching (s) and bending (b) components of the nearest-neighbor force-constant tensors for CuPd systems as a function of bond length. The figure illustrates that the linear fitting is appropriate for the present case as the monotonic decrease in the force constants with the increasing bond distances is well captured for all three pairs of interatomic force constants. The computed values of correlation coefficients for the straight-line fitting of stretching components of the force constant tensors varies between 0.96 and 0.98 which shows the fit to be very good. The fit accuracy for the bending components is, however, a bit low with the calculated correlation coefficient varies between 0.65 and 0.87. This, however, is acceptable, as the bending components of force-constant matrices are order of magnitude smaller than the stretching components and therefore, play minimal role in affecting the results. The stretching and bending force constants for the alloy $Cu_{0.715}Pd_{0.285}$ at its experimental bond length, obtained from the fitted results, are presented in Table II. The results show that the Cu-Cu and the Cu-Pd force constants are much softer than that of the Pd-Pd ones, with the Cu-Cu force constants being the softest. This is only to be expected as the equilibrium Pd-Pd bond length in pure Pd (5.32 a.u.) is significantly larger than that in this alloy, thus making the Pd-Pd bonds stiffer than the other kinds in the alloy environment where the volume available for the Pd atoms is much less compared to pure Pd.

TABLE II. Computed s and b force constants, in units of dyne per centimeter for $Cu_{0.715}Pd_{0.285}$ using "bond stiffness vs bond-length approach."

Pair type	Bond length (a.u.)	s	b
Cu-Cu[a]	4.9695	24610.62	−1312.64
Pd-Pd[a]	4.9695	67824.28	−2511.19
Cu-Pd[a]	4.9695	43582.46	−1803.09
Cu-Cu[b]	4.989	23981.67	−1289.29
Pd-Pd[b]	5.10	58285.63	−2372.90
Cu-Pd[b]	5.037	37793.93	−1528.49

[a]No relaxation is considered.
[b]Relaxation is incorporated.

In what follows, we use the transferable force constants of Table II as inputs to the ICPA and calculate the phonon-dispersion curves for the alloy which are presented in the top panel of Fig. 2. It can be seen that the calculated and experimental results of phonon frequencies agree reasonably well except near the zone edges where a frequency shift in the dispersion curves is observed in the longitudinal branches along all the symmetry directions. This is a typical resonancelike behavior at around $\nu=6.65$ THz associated with a large density of states contributed by the Pd atoms. This kind of frequency shift in the dispersion curves, which is altogether absent in the experimental results is generally associated with a very strong force-constant disorder and is seen in the past for some other alloys too (for example, Ni-Pt alloy[5]). To find out whether the disorder in the force constants is the possible reason for this anomalous frequency shift obtained from our calculations, we look into the partial and the total structure factors and try to understand the contributions of each pair of species toward the normal modes. In Fig. 3, we

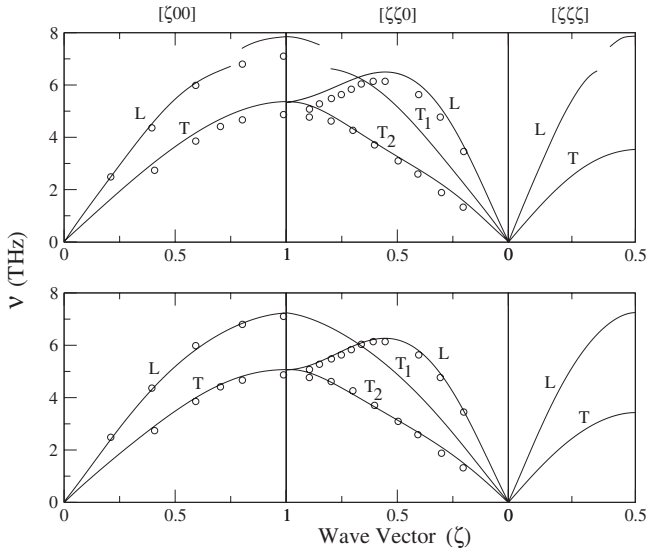

FIG. 2. Dispersion curves (frequency ν vs reduced wave vector ζ); $\zeta=\frac{|\vec{q}|}{|\vec{q}_{max}|}$, $\vec{q}$ the phonon wave vector; for $Cu_{0.715}Pd_{0.285}$ calculated in the ICPA (solid lines). The upper panel corresponds to the results obtained with the force constants extracted at the alloy bond length (4.9695 a.u.) using "bond stiffness vs bond-length" method while the lower panel corresponds to the results obtained with the force constants obtained at the relaxed bond lengths (mentioned in Table II) using the same method. The circles are the experimental data.

present results for the structure factors along $[\zeta,0,0]$ direction and for the longitudinal branch at some selected ζ values. No anomalous behavior is observed for wave vectors up to $\zeta=0.7$ with a single distinct peak in the structure factors. However, near [0.75,0,0], the peaks due to Cu-Pd and Pd-Pd tend to shift toward higher frequency region, whereas, the Cu-Cu peak remains static at a lower frequency. This in turn increases the phonon linewidth and the line becomes gradually asymmetric in shape. This scenario is portrayed more

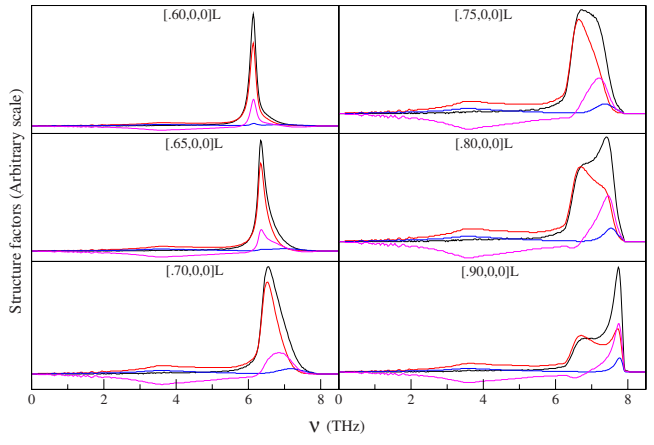

FIG. 3. (Color online) Partial and total structure factors calculated by the ICPA for various ζ values in the $[\zeta,0,0]$ direction in $Cu_{0.715}Pd_{0.285}$ with force constants calculated at the alloy bond length. The black lines are the total contributions, the red lines are the Cu-Cu contributions, the blue lines are the Pd-Pd contributions, and the magenta lines are the Cu-Pd contributions. All the curves are for longitudinal modes.

clearly in the structure factors for [0.80,0,0] and [0.90,0,0] where the peak position of the phonon line is shifted to a high-frequency value with a small shoulder remaining in the low-frequency side which is entirely due to the contribution from the Cu-Cu pair. This behavior must be responsible for the jump in frequency in the phonon-dispersion curves near the zone boundary. It can be stated in this context that the peak position at high wave vectors is dominated by Cu-Pd pair with some contribution from Pd-Pd pair which indicates that Cu-Pd and Pd-Pd force constants are overestimated in the present case leading to the anomalous splitting in the dispersion curves. Hence, these set of force constants do not depict the correct nature of bond stiffness's in this alloy. This spurious effect was earlier observed in case of Fe-Pd alloys where a erroneous estimation of interatomic force constants in random environment led to anomalous splitting of phonon branches and the origin of such anomaly could be understood based upon an analysis of partial and total structure factors.[13,21]

As already discussed, the size mismatch of the constituent elements should have a significant effect on the vibrational properties of an alloy. As the alloy expands (or contracts) locally on introduction of disorder into the system, the lengths of all chemical bonds decrease (or increases) affecting the stiffness's of the corresponding bonds. For $Cu_{0.715}Pd_{0.285}$, it can be observed from Table I that there is notable size difference between Cu and Pd in their elemental phases. Therefore, using the force constants for all three types of bonds at the experimental bond length of the alloy, we have neglected the local relaxations around atoms of different sizes forcing overstiffening of the bonds involved with larger Pd atoms. Thus, to address the real nature of microscopic interactions among various pairs of specie in the alloy, it is essential to incorporate the lattice relaxation effects into our scheme of calculations. In this regard, Mousseau and Thrope[29] had performed a study on bond-length distribution associated with a pair of chemical specie with compositions for a number of fcc-based binary metallic alloys which included Cu_xPd_{1-x} as well. It had been observed by the authors of Ref. 29 that in our coveted alloy, the nearest-neighbor bond distances between different pairs of specie differ a lot from the average or mean bond distance. We have estimated the relative variation in bond lengths for each pair with respect to the mean distance as mentioned in the paper and introduced the same in our calculation. The new relaxed bond lengths are being worked out by incorporating the same relative changes as per the above scheme to our computed mean distance which is about 5.0277 a.u. The relaxed bond lengths and the corresponding force constants are presented in Table II for comparison. It is observed that the bond lengths involving the larger Pd atoms are larger than the average bond length while there is a contraction of the lattice in the neighborhood involving Cu atoms only. Consequently, the Cu-Pd and Pd-Pd force constants reduce by a significant amount compared to the unrelaxed lattice force constants while the Cu-Cu ones remain almost unaltered because of very minimal change in Cu-Cu bond distances with respect to the unrelaxed lattice. This indicates that on incorporation of lattice relaxation into our calculation, the Cu-Pd and Pd-Pd interactions soften noticeably. To see whether this re-

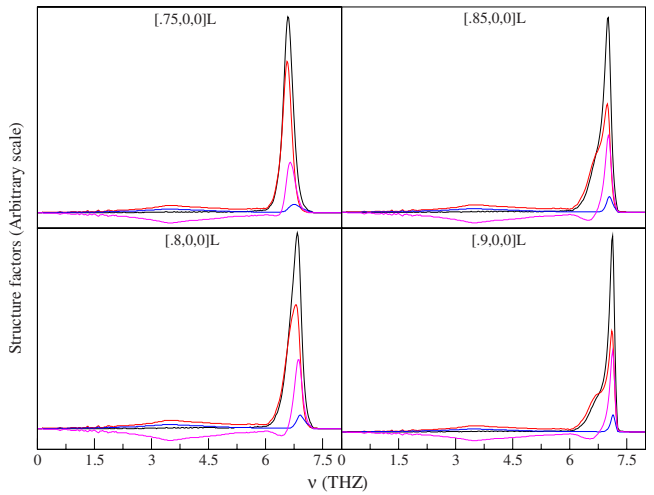

FIG. 4. (Color online) Partial and total structure factors calculated by the ICPA for various ζ values in the $[\zeta,0,0]$ direction in $Cu_{0.715}Pd_{0.285}$ with force constants calculated at the relaxed bond lengths. The black lines are the total contributions, the red lines are the Cu-Cu contributions, the blue lines are the Pd-Pd contributions, and the magenta lines are the Cu-Pd contributions. All the curves are for longitudinal modes.

laxation gets rid of the spurious frequency shift in the phonon-dispersion curves, we plot the dispersion curves with the new set of force constants in the bottom panel of Fig. 2 and the corresponding structure factors in Fig. 4. The results of phonon frequencies in the bottom panel of Fig. 2 show that the shift in frequency as observed in the previous case in the top panel of the same figure has disappeared completely and an excellent agreement between the theoretical and experimental results is obtained. To understand the reason, we look into the partial and total structure factors for the longitudinal branch along $[\zeta,0,0]$ direction in Fig. 4. Here, no sudden shift in the peak position is observed around $\zeta=0.75$ because the peaks in the structure factors from all three pairs of specie occur at the same frequencies, unlike the case with the unrelaxed lattice where the overstiffening of the bonds involving Pd atoms shifted the contributions from Cu-Pd and Pd-Pd pairs toward higher frequencies. Hence, we conclude that apart from the mass and the force-constant disorders, the local lattice relaxation and thus the environmental effects play an important role in the Cu_xPd_{1-x} alloy and one must consider it in an appropriate manner to understand the lattice dynamics of the system properly. The first-principles based TFC-ICPA model has, thus, been successful in not only obtaining the accurate dispersion relations but also in interpreting the microscopic picture leading to it.

B. $Cu_{0.75}Au_{0.25}$

Next, we discuss the Cu-Au alloy where several experimental and theoretical investigations[30–32] in the low concentration limits of Cu have been reported. Previous studies on this system revealed that the lattice constant changes substantially with changes in compositions which implies a variation in the interatomic force constants even between the like atoms in the alloy environment with respect to the pure

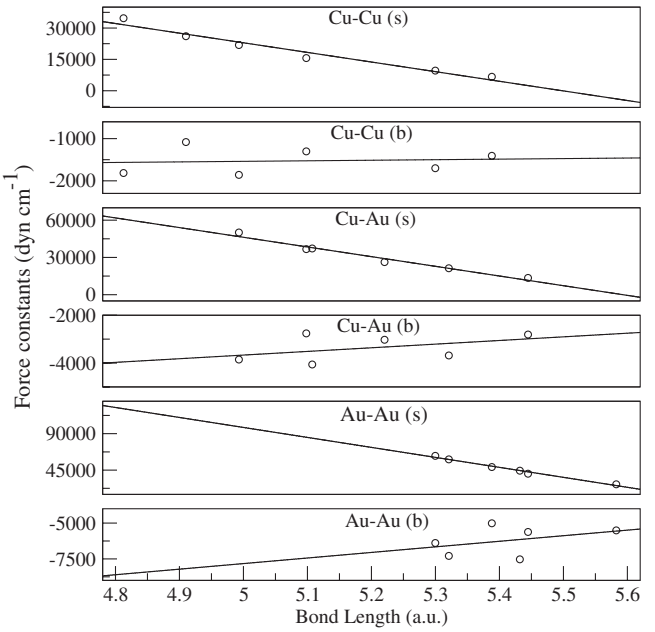

FIG. 5. Nearest-neighbor s and b force constants for Cu_xAu_{1-x} as a function of bond length. The solid lines are the fitted functions whereas the circles correspond to data obtained from *ab initio* calculations on one of a set of structures ($L1_2$ at four different volumes, $L1_0$ at two different volumes, fcc Cu and fcc Au at two different volumes.)

elements. To begin with, we present in Fig. 5, the s and b components of the nearest-neighbor force constant tensors for CuAu as a function of bond length. As was the case with the CuPd, the linear fitting is found to be appropriate for the present case. The stretching and bending components of the force-constant tensors for the alloy $Cu_{0.75}Au_{0.25}$ at its experimental bond length obtained from the fitted results are presented in Table III. The Au-Au force constants are about 300% larger in magnitude than that of the Cu-Cu ones, whereas, the Cu-Au ones are on an average 100% larger than

TABLE III. Computed force constants, in units of dyne per centimeter for $Cu_{0.75}Au_{0.25}$ using bond stiffness vs bond-length approach.

Pair type	Bond length (a.u.)	s	b
Cu-Cu[a]	5.0098	22486.36	−1537.38
Au-Au[a]	5.0098	96460.75	−7788.05
Cu-Au[a]	5.0098	45481.08	−3651.43
Cu-Cu[b]	5.0065	22639.54	−1537.81
Au-Au[b]	5.2523	66595.32	−6844.91
Cu-Au[b]	5.0788	40107.48	−3546.24
Cu-Cu(expt.)		34890.00[c]	−3060.00[c]
Au-Au(expt.)		34890.00[c]	−3060.00[c]
Cu-Au(expt.)		34890.00[c]	−3060.00[c]

[a]No relaxation is considered.
[b]Relaxation is incorporated.
[c]Reference 9.

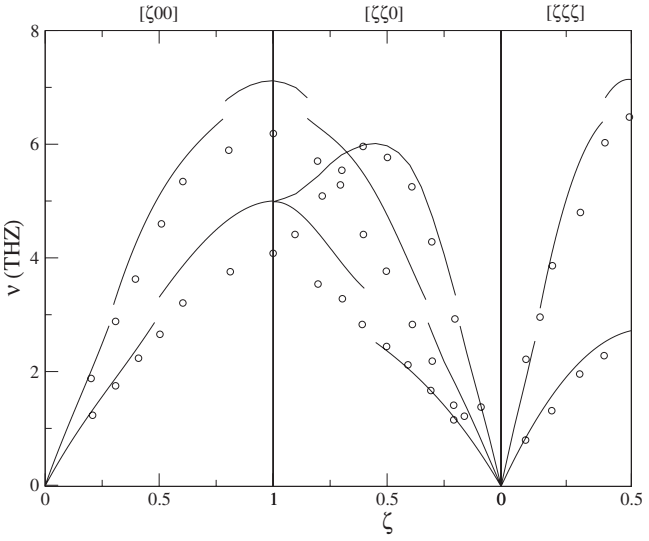

FIG. 6. Dispersion curves (frequency ν vs reduced wave vector ζ); $\zeta=\frac{|\vec{q}|}{|\vec{q}_{\max}|}$, $\vec{q}$ the phonon wave vector; for $Cu_{0.75}Au_{0.25}$ calculated in the ICPA (solid lines) with the force constants obtained at the alloy bond length (5.0098 a.u.) using bond stiffness vs bond-length method. The circles are the experimental data.

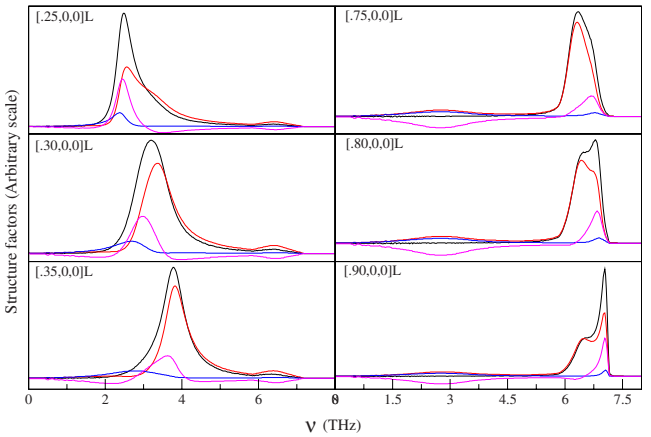

FIG. 7. (Color online) Partial and total structure factors calculated by the ICPA for various ζ values in the $[\zeta,0,0]$ direction in $Cu_{0.75}Au_{0.25}$ with force constants calculated at the alloy bond length. The black lines are the total contributions, the red lines are the Cu-Cu contributions, the blue lines are the Au-Au contributions, and the magenta lines are the Cu-Au contributions. All the curves are for longitudinal modes.

the corresponding Cu-Cu force constants. This represents a situation of huge mass and force-constant disorder and one should anticipate significant effect of these disorders on the phonon-dispersion curves. The huge differences in the magnitude of force constants must be an artifact of forcing the larger Au atoms to vibrate in a lattice much smaller compared to the equilibrium lattice of Au in its elemental phase (bond length=5.58 a.u.). As a result of this, Au-Au bonds get stiffer. The Cu-Cu bond stiffness, on the other hand, do not differ significantly from that found in $Cu_{0.715}Pd_{0.285}$ because of the comparable Cu-Cu bond lengths in both cases. The phonon-dispersion curve for the alloy is presented in Fig. 6. A resonance behavior is observed around $\nu=2.9$ THz for all the branches except the $[\zeta,\zeta,\zeta]$T branch. In addition to that a secondary resonance is observed around $\nu=6.65$ THz only along the longitudinal branch for all the symmetry directions. This kind of secondary resonance is previously observed in Ni_xPt_{1-x}, characterized by a high density of phonon states near the resonance frequency, and for the similar concentration ratio of larger and smaller atom.[5] However, the experimental results available for the present alloy do not show any signature of resonancelike behavior. This is somewhat puzzling as the mass and size ratio between the constituent elements in Ni_xPt_{1-x} is almost identical as that of Cu_xAu_{1-x} alloy and hence, one should expect similar qualitative features in both the alloys. To find out the possible reasons of the discrepancy between the theoretical and the experimental results, we investigate the partial and the total structure factors and analyze the role played by each specie pair toward the normal modes. In Fig. 7, we present the structure factors for the longitudinal branch at some relevant reduced wave vectors along $[\zeta,0,0]$ direction. The left panel of the figure shows that at $\zeta=0.25$, the contributions to the structure factor from vibrations of all three pairs of atoms occur at same frequency, while at around $\zeta=0.3$ where the first resonance occurs, the contributions from the Cu-Cu pairs to the structure factor start to shift toward higher frequencies compared to the Au-Au and Cu-Au ones, thereby, increasing the phonon linewidth and producing asymmetric line shapes. At higher wave vectors, we again see a resonancelike behavior as a result of strong force-constant disorder. The right panel of Fig. 7 suggests that for wave vectors beyond $\zeta=0.75$, significant contributions from Cu-Au and Au-Au pairs start to buildup at frequencies higher than those where the vibrations from Cu-Cu pairs contribute. This moves the phonon peak positions at higher frequencies as can be clearly be seen by comparing the structure factors at $\zeta=0.75$ and at $\zeta=0.80$. This demonstrates the fact that the overestimations of the Cu-Au and the Au-Au force constants are responsible for this splitting of the dispersion curves at higher frequencies and hence, the force constants extracted at the experimental bond length of the alloy do not represent the correct nature of interatomic interactions in this alloy.

There is significant mass and size difference between Cu and Au atoms with the latter being the heavier and larger of the two as can be seen from Table I. This would most obviously result in an enhanced overlap of the heavy Au atoms with their nearest neighbors because of their larger size and the situation would be vastly different from that of a lattice with identical bond length for all the pairs of species. As a corrective measure, we adopt the same strategy as we have already successfully implemented for Cu-Pd system. Mousseau and Thrope, in their paper have shown the dispersion of bond lengths for various pairs of specie in the Cu_xAu_{1-x} alloy. As is done for the $Cu_{0.715}Au_{0.285}$ system, we incorporate the relative changes to our theoretically calculated average bond length which is about 5.0788 a.u. and get three distinct bond lengths for the three different pairs of specie in the alloy. Force constants corresponding to these new bond lengths are extracted from the fitted relationships of Fig. 5 and are presented in Table III. It can be seen that in comparison to the unrelaxed case, the Au-Au and the Cu-Au force

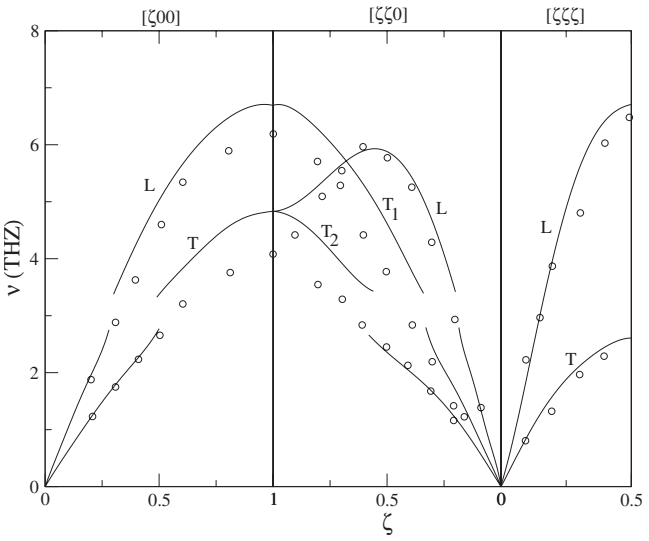

FIG. 8. Dispersion curves (frequency ν vs reduced wave vector ζ); $\zeta=\frac{|\vec{q}|}{|\vec{q}_{\max}|}$, $\vec{q}$ the phonon wave vector; for $Cu_{0.75}Au_{0.25}$ calculated in the ICPA (solid lines) with the force constants obtained at the new relaxed bond lengths (mentioned in Table III) using bond stiffness vs bond-length method. The circles are the experimental data.

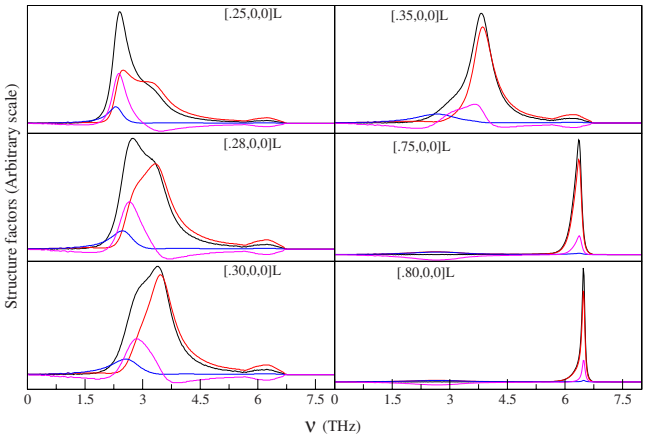

FIG. 9. (Color online) Partial and total structure factors calculated by the ICPA for various ζ values in the $[\zeta,0,0]$ direction in $Cu_{0.75}Au_{0.25}$ with force constants calculated at the relaxed bond lengths. The black lines are the total contributions, the red lines are the Cu-Cu contributions, the blue lines are the Au-Au contributions, and the magenta lines are the Cu-Au contributions. All the curves are for longitudinal modes.

constants have been softened by a large amount. On the other hand, the Cu-Cu force constants remain almost unchanged in comparison to the unrelaxed ones, as was the case for the Cu-Pd alloy. To study the effect of the relaxed environment involving the chemical bonds on the phonon spectra, we plot the dispersion curves obtained with the relaxed force constants in Fig. 8. It can be seen that the secondary resonancelike splitting in the dispersion curves has disappeared and that the frequencies near the zone boundary have shifted toward lower values in comparison to the unrelaxed case, thus improving the agreement between theory and experiment. This, thus is an artifact of the softer Cu-Au and Au-Au force constants due to the expansion of bonds associated with the Au atoms. However, the resonance mode at frequency around 2.9 THz still persists along $[\zeta,0,0]$ and $[\zeta,\zeta,0]$ directions, whereas, it is not observable along $[\zeta,\zeta,\zeta]$ direction which indicates a direction-dependent resonant behavior. For deeper analysis, we look into the partial and the total structure factors for the longitudinal branch along $[\zeta,0,0]$ direction in Fig. 9. For lower values of ζ and around the resonance, we see no qualitative difference between the unrelaxed case and the relaxed case. For higher ζ values, we observe that the contributions from all three pairs occur at the same frequency, unlike the unrelaxed case. These suggest that the resonancelike behavior at higher ζ values stem from the overstiffening of the bonds involving bigger Au atoms and that the incorporation of relaxations took care of it. However, the resonance behavior at lower ζ region has no correlation with the local lattice relaxations. Thus, in spite of the incorporation of bond relaxations improving the agreement between theoretically calculated and experimentally observed phonon-dispersion curves, the qualitative difference because of the existence of a resonance mode at around $\nu=2.9$ THz is still an enigma that has to be resolved. Katano *et al.* in Ref. 9 had performed a fourth neighbor Born-von Karman fit to the experimentally measured phonon frequencies and extracted the interatomic force constants. Surprisingly, they achieved an excellent fit to the experimental results using this model which only assumes an average rigid lattice and neglect any mass and force-constant fluctuations. This was quite a puzzle because it suggested that the large mass and size ratio had little effect on the phonon frequencies. In an attempt to solve the above puzzle, we have carried out calculations with the CPA which assumes fluctuations in mass only and the virtual-crystal approximation (VCA) which assumes a rigid lattice with average mass and average force constants throughout the sample, using force constants as reported by Katano *et al.*[9] in both calculations. Our motivation behind this is to systematically explore the effect of each type of disorder on phonon spectra starting from the average lattice (no disorder) and thus understand the reason behind the success of the "average lattice model" for a system supposed to have strong disorders in mass, force constants, and environment. The force constants for the nearest neighbors as obtained by the fit to the experimental frequency is listed in Table III for comparison. Figure 10 shows that an excellent agreement between theory and experiment for all the symmetry directions is achieved using the VCA. However, the same qualitative disagreement between the theory and the experimental results that was observed in case with mass and force-constant disorders on a relaxed lattice (Fig. 8) persists in case of calculations with the CPA as well, shown in Fig. 11. Quantitatively, the results with the CPA are far worse than those obtained with the ICPA on a relaxed lattice. In the long-wavelength region, the CPA calculated frequencies are substantially underestimated in comparison to the experimentally observed values, whereas, for high wave vectors the calculated frequencies are significantly overestimated in comparison to the experimental ones. This result, thus, suggests that both the mass and the force-constant disorder have significant role in the lattice dynamics in this system and thus, neglecting any one of them would

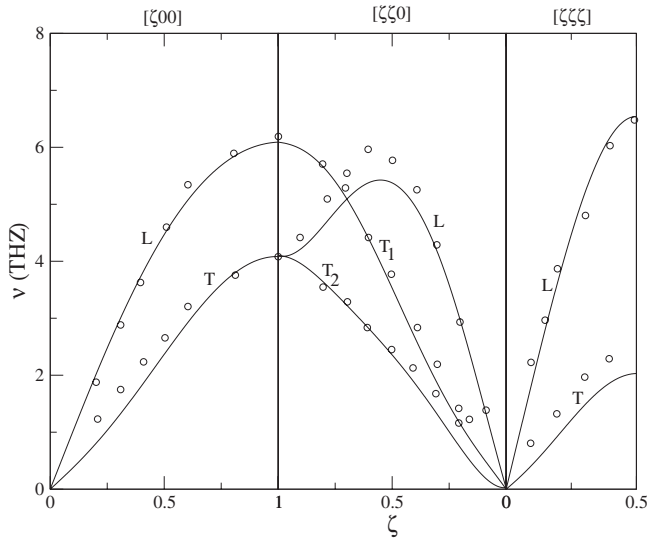

FIG. 10. Dispersion curves (frequency ν vs reduced wave vector ζ); $\zeta=\frac{|\vec{q}|}{|\vec{q}_{\max}|}$, $\vec{q}$ the phonon wave vector; for $Cu_{0.75}Au_{0.25}$ calculated in the VCA (solid lines) with the force constants obtained by fitting experimental frequencies to the Born-von Karman model (mentioned in Table III) using bond stiffness vs bond-length method. The circles are the experimental data.

provide a qualitatively wrong picture of the microscopic physics. This can be realized more clearly from CPA results. For high wave vectors and thus higher frequencies, the normal modes would be dominated by the vibrations of lighter Cu atoms. For low wave vectors and lower frequencies, heavier Au atoms will contribute most toward the normal modes. The average force constants used in the CPA calculations are way too large compared to the Cu-Cu force constants obtained by the TFC upon considering local lattice relaxations. This, therefore, pushes the frequencies further up at higher wave vectors. On the other hand, the Au-Au force constants obtained by the TFC incorporating relaxations are much larger than the average force constants. Thus, in the low wave-vector region, the CPA calculated frequencies are pulled down. In the VCA or the average lattice model, the average mass used, is higher (lower) than the mass of Cu (Au). A higher (lower) mass in the high (low) wave-vector region, in comparison to the CPA, compensates for the stiffer (softer) bonds, and thus pulls the frequencies down (up) making a perfect agreement with the experiments. This points to the fact that the error introduced due to consideration of an average mass is compensated by the erroneous set of force constants; a classic case of cancellation of errors leading to perfect agreement with experiments.

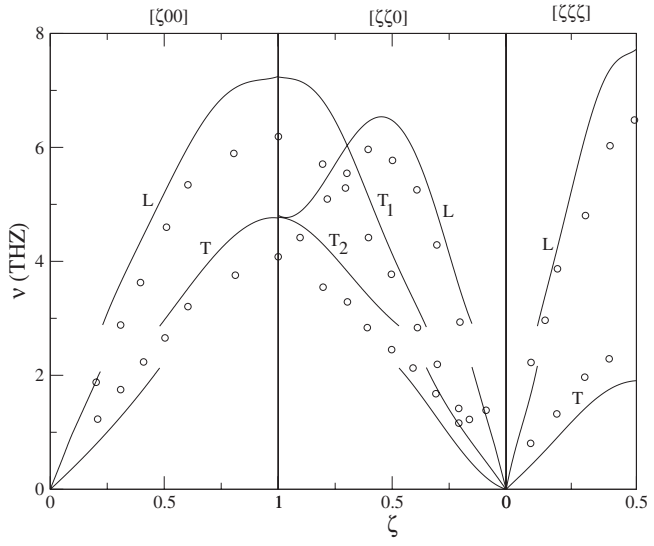

FIG. 11. Dispersion curves (frequency ν vs reduced wave vector ζ); $\zeta=\frac{|\vec{q}|}{|\vec{q}_{\max}|}$, $\vec{q}$ the phonon wave vector; for $Cu_{0.75}Au_{0.25}$ calculated in the CPA (solid lines) with the force constants obtained by fitting experimental frequencies to the Born-von Karman model (mentioned in Table III) using bond stiffness vs bond-length method. The circles are the experimental data.

These results, thus, clearly show that the mass disorder, the force-constant disorder, and the local lattice relaxations, together make up the phonon dispersions in this alloy, being correctly addressed by the first-principles based TFC-ICPA method and that the nonappearance of the resonance mode in the experiments could be due to the limitations in the measurements. These propositions have solid grounds because of the fact that the similar branch-dependent resonance modes have been experimentally observed for $Cu_{0.97}Au_{0.03}$ (Ref. 31) and $Cu_{0.91}Au_{0.09}$.[30] Large values of natural line widths which contain information about the disorder effects were observed in these systems around a frequency of 2.6 THz, the resonance frequency. A mass disorder only theory for impurities, although worked reasonably well for $Cu_{0.97}Au_{0.03}$, failed to explain the frequency shifts and large disorder-induced widths near the resonance frequency,[30] thus indicating that the fluctuations in force constant are a must to understand the phonon spectra in these alloys. Thus, the resonance behavior in $Cu_{0.75}Au_{0.25}$ is expected. To further validate our arguments, we have calculated the disorder-induced widths. Results for the longitudinal branch along $[\zeta,0,0]$ direction for $Cu_{0.75}Au_{0.25}$ are shown in the top panel of Fig. 12. Results for the $Cu_{0.715}Pd_{0.285}$ system are also shown for comparison. The behavior of the widths are similar for other directions and thus we refrain from showing them. It can be seen in Fig. 12 that at around $\nu=2.9$ THz, an anomalously large width is observed in case of $Cu_{0.75}Au_{0.25}$, coinciding with the region where the resonance occurs. No such anomalously large width is obtained for $Cu_{0.715}Pd_{0.285}$ which indicates the absence of a resonance mode. That this anomalously large width is indeed a signature of the resonance mode is further reinforced by the results on the vibrational densities of states. In case of alloys made up by the heavier impurity in a lighter host, the states with lower frequencies are dominated by the heavier atoms which gradually merge with the main host band. However, the occurrence of resonance in such alloys is marked by a large density of states of the heavier atoms near the resonance frequencies and subsequent decay of the states into the main host band. This extra scattering induced by the impurity atoms in the host band produces a large width near the resonance frequency. The bottom panel of Fig. 12 shows the vibrational densities of states of these two systems under considerations. Around the resonance frequency according to our calculations, the $Cu_{0.75}Au_{0.25}$ system has larger densities of states as compared to that of $Cu_{0.715}Pd_{0.285}$. The large con-

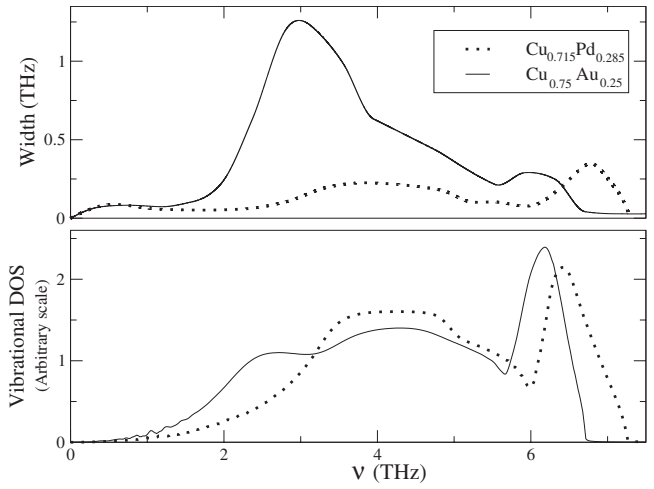

FIG. 12. Top panel shows the disorder-induced widths in $Cu_{0.75}Au_{0.25}$ (solid line) and in $Cu_{0.715}Pd_{0.285}$ (dotted line) along $[\zeta,0,0]$ direction for the longitudinal branch calculated in the ICPA using the force constants obtained at their respective relaxed bond lengths. The corresponding vibrational densities of states for $Cu_{0.75}Au_{0.25}$ (solid line) and $Cu_{0.715}Pd_{0.285}$ (dotted line) are presented in the bottom panel.

tributions are all due to the heavier Au states which form a broad peak between 2.5 and 3 THz before decaying into the host Cu band. Such a phenomena has been observed in the past for Ni_xPt_{1-x} alloys,[5] a system with similar degree of mass and force-constant disorder as $Cu_{0.75}Au_{0.25}$. In case of $Cu_{0.715}Pd_{0.285}$ alloy, we do not observe any broad peak in the densities of states in the low-frequency part of the spectrum and the densities of states curve looks more like that of pure Cu. The absence of any such peak in the vibrational densities of states along with the absence of an anomalously large linewidth in the low-frequency part of the spectrum in $Cu_{0.715}Pd_{0.285}$ can be attributed to the lesser mass and size ratio of the constituents in this alloy compared to that in $Cu_{0.75}Au_{0.25}$ and is the reason behind the qualitative differences in the phonon-dispersion relations between these two systems.

IV. CONCLUSIONS

The role of size mismatch of the end-point components on lattice dynamics of binary alloys has been investigated by a combination of first-principles density-functional perturbation theory, the TFC model for accurate computation of force constants and the ICPA method for configuration averaging in disordered environment. On incorporation of bond-length fluctuations for the alloy $Cu_{0.715}Pd_{0.285}$, the phonon-dispersion curves agree very well with the experimental results. In case of $Cu_{0.75}Au_{0.25}$ we find a resonance mode at around 2.9 THz which is not observed in the experiments. A systematic investigation reveals that this alloy presents a case where both the mass and the force-constant disorders play significant role in determining the phonon frequencies. The good agreement obtained with the average mass and average set of force constants extracted by fitting the experimental frequencies to a Born-von Karman model, is indicative of cancellation of errors emanating from the nonincorporation of the fluctuations in mass and from the nonincorporation of the disorder in the interatomic force constants. Presence of resonance modes in the experimental results for the Cu-Au alloy at even smaller concentrations of Au suggest that the results obtained by us with relaxed bond lengths indeed capture the real picture of complex interplay of various types of disorders influencing the phonon dispersions in $Cu_{0.75}Au_{0.25}$ and that a more careful experiment has to be performed so as to produce the disorder-induced effects properly for this alloy.

ACKNOWLEDGMENT

One of the authors (B.D.) would like to acknowledge CSIR, India for financial support under the Grant-F. No. 09/731(0049)/2007-EMR-I.

*b.dutta@iitg.ernet.in
†konark@iitg.ernet.in
‡subhra@iitg.ernet.in

[1] P. Bruesch, *Phonon, Theory and Experiment* (Springer-Verlag, New York, 1982).
[2] P. D. Bogdanoff and B. Fultz, Philos. Mag. B **79**, 753 (1999).
[3] A. van de Walle and G. Ceder, Phys. Rev. B **59**, 14992 (1999).
[4] A. van de Walle and G. Ceder, Phys. Rev. B **61**, 5972 (2000).
[5] Y. Tsunoda, N. Kunitomi, N. Wakabayashi, R. M. Nicklow, and H. G. Smith, Phys. Rev. B **19**, 2876 (1979).
[6] Y. Noda, D. K. Saha, and K. Ohshima, J. Phys.: Condens. Matter **5**, 1655 (1993).
[7] Y. Noda, K. Ohshima, and Y. Endoh, Physica B **219**, 490 (1996).
[8] E. D. Hallman, Can. J. Phys. **52**, 2235 (1974).
[9] S. Katano, M. Iizumi, and Y. Noda, J. Phys. F: Met. Phys. **18**, 2195 (1988).
[10] S. Ghosh, P. L. Leath, and M. H. Cohen, Phys. Rev. B **66**, 214206 (2002).
[11] D. W. Taylor, Phys. Rev. **156**, 1017 (1967).
[12] S. Ghosh, J. B. Neaton, A. H. Antons, M. H. Cohen, and P. L. Leath, Phys. Rev. B **70**, 024206 (2004).
[13] A. Alam, S. Ghosh, and A. Mookerjee, Phys. Rev. B **75**, 134202 (2007).
[14] P. Hohenberg and W. Kohn, Phys. Rev. **136**, B864 (1964).
[15] W. Kohn and L. J. Sham, Phys. Rev. **140**, A1133 (1965).
[16] S. Baroni, S. De Gironcoli, A. Dal Corso, and P. Giannozzi, Rev. Mod. Phys. **73**, 515 (2001).
[17] A. van de Walle, Ph.D. thesis, MIT, 2000.
[18] E. J. Wu, G. Ceder, and A. van de Walle, Phys. Rev. B **67**, 134103 (2003).
[19] J. Z. Liu, G. Ghosh, A. van de Walle, and M. Asta, Phys. Rev. B **75**, 104117 (2007).
[20] A. van de Walle and G. Cedar, Rev. Mod. Phys. **74**, 11 (2002).
[21] B. Dutta and S. Ghosh, J. Phys.: Condens. Matter **21**, 395401

(2009).
[22] D. H. Dutton, B. N. Brockhouse, and A. P. Miller, Can. J. Phys. **50**, 2915 (1972).
[23] J. W. Lynn, H. G. Smith, and R. M. Nicklow, Phys. Rev. B **8**, 3493 (1973).
[24] P. Giannozzi, S. Baroni, N. Bonini, M. Calandra, R. Car, C. Cavazzoni, D. Ceresoli, G. L. Chiarotti, M. Cococcioni, I. Dabo, A. Dal Corso, S. de Gironcoli, S. Fabris, G. Fratesi, R. Gebauer, U. Gerstmann, C. Gougoussis, A. Kokalj, M. Lazzeri, L. Martin-Samos, N. Marzari, F. Mauri, R. Mazzarello, S. Paolini, A. Pasquarello, L. Paulatto, C. Sbraccia, S. Scandolo, G. Sclauzero, A. P. Seitsonen, A. Smogunov, P. Umari, and R. M. Wentzcovitch, J. Phys.: Condens. Matter **21**, 395502 (2009).
[25] D. Vanderbilt, Phys. Rev. B **41**, 7892 (1990).
[26] S. G. Louie, S. Froyen, and M. L. Cohen, Phys. Rev. B **26**, 1738 (1982).
[27] J. P. Perdew, K. Burke, and M. Ernzerhof, Phys. Rev. Lett. **77**, 3865 (1996).
[28] M. Methfessel and A. T. Paxton, Phys. Rev. B **40**, 3616 (1989).
[29] N. Mousseau and M. F. Thorpe, Phys. Rev. B **45**, 2015 (1992).
[30] E. C. Svensson, B. N. Brockhouse, and J. M. Rowe, Solid State Commun. **3**, 245 (1965).
[31] E. C. Svensson and B. N. Brockhouse, Phys. Rev. Lett. **18**, 858 (1967).
[32] E. C. Svensson and W. A. Kamitakahara, Can. J. Phys. **49**, 2291 (1971).